



Daily soil temperature modeling improved by integrating observed snow cover and estimated soil moisture in the U.S. Great Plains

Haidong Zhao¹, Gretchen F. Sassenrath^{2,3}, Mary Beth Kirkham³, Nenghan Wan¹, Xiaomao Lin^{1*}

5

¹Department of Agronomy, Kansas Climate Center, Kansas State University, Manhattan, Kansas, USA

²Southeast Research and Extension Center, Parsons, Kansas, USA

³Department of Agronomy, Kansas State University, Manhattan, Kansas, USA

10 *Correspondence to:* X. Lin (xlin@ksu.edu)



Abstract

15 Soil temperature (T_s) plays a critical role in land-surface hydrological processes and agricultural ecosystems. However, soil temperature data are limited in both temporal and spatial scales due to the configuration of early weather station networks in the U.S. Great Plains. Here, we examined an empirical model (EM02) for predicting daily soil temperature (T_s) at the 10 cm depth across Nebraska, Kansas, Oklahoma, and parts of Texas that comprise the U.S. winter wheat belt. An improved empirical
20 model (iEM02) was developed and calibrated using available historical climate data prior to 2015 from 87 weather stations. The calibrated models were then evaluated independently using the latest 5-year observations from 2015 to 2019. Our results suggested that the iEM02 had, on average, an improved root mean square error (RMSE) of 0.6°C for 87 stations when compared to the original EM02 model. Specifically, after incorporating changes in soil moisture and daily snow depth, the improved model
25 was 50% more accurate as demonstrated by the decrease in RMSE. We conclude that in the U.S. Great Plains the iEM02 model can better estimate soil temperature at the surface soil layer where most hydrological and biological processes occur. Both seasonal and spatial improvements made in the improved model suggest that it can provide a daily soil temperature modeling tool that overcomes the deficiencies of soil temperature data used in assessments of climatic changes, hydrological modeling,
30 and winter wheat production in the U.S. Great Plains.



1 Introduction

A reliable estimate of soil temperature (T_s) is useful to understand agricultural ecological systems, hydrological processes, and land-atmosphere interactions (Lembrechts et al., 2020; Qi et al., 2016; Zhang et al., 2018) due to the fact that T_s governs physical, chemical, and biological processes of the soil and interactions between the atmosphere and land-surface (Smith, 2000; Soong et al., 2020). In particular, T_s has been widely used for a better understanding of changes in soil moisture (Lakshmi et al., 2003), the ecosystem carbon balance (Goulden et al., 1998), and the nitrogen mineralization process (Persson and Wirén, 1995) although a larger prevalence of air temperature observations are available as a soil temperature proxy. From a practical perspective, T_s is critical for agricultural system models such as the crop environmental resource synthesis (CERES) models to assess the impacts of extreme climate on crop production and stress tolerance, thereby allowing producers to better prepare for proactive and reactive field management (Bergjord et al., 2008; Persson et al., 2017; Williams et al., 1989). Frequent extreme climate events such as spring freezes and summer heat stress can impact winter wheat [*Triticum aestivum* L.] growth and development, reducing grain yields by more than 7% in the U.S. winter wheat belt (Tack et al., 2015; Paulsen and Heyne, 1983). These effects are also modulated through land-surface interaction processes (Hillel, 1998; Araghi et al., 2017).

To improve the accuracy of crop management modeling, a bare soil temperature (T_s) at the 10 cm depth, a standard soil temperature variable, has commonly been considered as a more direct and useful variable than air temperature (T_a) measured at 1.5 or 2 m height in crop phenology (Onwuka and Mang, 2018), plant photosynthesis and soil respiration (Meyer et al., 2018; Wu and Jansson, 2013), plant



nutrient uptake (Yan et al., 2012), and estimate of crop production (Araghi et al., 2017; Hillel, 1998). There are many T_s modeling techniques mostly based on the land-surface interaction process (Qi et al., 2019; Yener et al., 2017). Most T_s models are rooted in theories of soil heat exchange and surface energy balance (Rankinen et al., 2004; Nobel and Geller, 1987; Chalhoub et al., 2017). The theory-based simulation for surface energy balance usually includes solar radiation (incoming and outgoing), infrared radiation (absorbed and reflected), turbulent flux energy (latent heat and sensible heat), and net ground heat flux through the ground surface into soil layers thermodynamically (Mihalakakou et al., 1997; Chalhoub et al., 2017). Obviously, the energy-balance based model usually requires more detailed near-surface and soil variables such as turbulent flux quantities (sensible heat flux and latent heat flux) to make the model reliable and accurate; however, determining quality turbulent flux quantities is not a trivial task (Kutikoff et al., 2021; Dhungel et al., 2021). In addition, seasonal variations of soil thermal conductivity and underestimates of actual evapotranspiration usually lead to overestimated surface soil temperatures (Bittelli et al., 2008). Therefore, simpler empirical models with fewer dynamic processes needed to predict T_s have been explored (Zheng et al., 1993; Plauborg, 2002; Liang et al., 2014; Badache et al., 2016; Kang et al., 2000). However, these empirical models might result in relatively large estimated errors of over 2°C due to the lack of details about physical process such as uncertainties of the soil volumetric heat capacity and thermal conductivity (Badía et al., 2017). For example, the volumetric heat capacity was higher for a clay soil, which ranged between 1.48 and 3.54 MJ m⁻³ °C⁻¹, than for a sand soil, which ranged between 1.09 and 3.04 MJ m⁻³ °C⁻¹ when the soil moisture content was between 0 to 0.25 kg kg⁻¹ (Abu-Hamdeh, 2003).



Currently, the U.S. Department of Agriculture (USDA) provides a high-resolution Gridded Soil Survey Geographic (gSSURGO) Database product (<https://gdg.sc.egov.usda.gov/>) that includes static soil
75 physical property data at 10 km resolution (USDA NRCS, 2013). The gSSURGO data facilitate T_s modeling, especially for better performance in large-scale T_s modeling due to its spatial variations in soil properties and soil moisture (USDA NRCS, 2013). These datasets have been widely used in the estimation of root-zone soil water content (Miller et al., 2018) and sub-surface hydrologic properties (Dirmeyer and Norton, 2018). The empirical model proposed by Plauborg (2002) performed better than
80 energy-balance based models when applied in the U.S. Great Plains for the last five years. Due to the lack of information about static soil properties on a large scale one or two decades ago, either over- or underestimates of T_s occurred, which gave a large deviations in the assessment of crop stress and crop production (Gupta et al., 1990; Stone et al., 1999).

85 Recent studies have shown that estimated soil temperature usually deviates from observed soil temperature in the winter due to snow cover, frozen soil, and wide spatial and temporal heterogeneity in frozen soil properties (Nagare et al., 2012; Zhang et al., 2008; Rankinen et al., 2004). The impact of snow cover on soil temperature has been investigated (Rankinen et al., 2004) and is partially accounted for by incorporating correcting factors in land-surface modeling as well as ecosystem models (Zhang et al., 2008) and soil and water assessment tools (SWAT) (Qi et al.2019). For both empirically and
90 physically-based soil temperature modules embedded in SWAT, the predictions of soil temperature in regions with thick snow cover seldom agree with field measurements in winter (Qi et al. 2019).



In the U.S. Great Plains, there has been increasing interest in improving hydrological process modeling of surface water and groundwater due to the Ogallala aquifer's depletion in recent decades (Haacker et al., 2019). However, observed soil temperature information has been provided by the automated weather station networks in this region that was commissioned in the late 1980s and early 1990s (Brock and Crawford, 1995). Not only were there few continuous observations for T_s earlier than the 1990s, these automated weather station networks also had limited stations in each state of the U.S. Great Plains. Such a lack of reliable soil temperature data both spatially and temporally makes the long-term assessment of water resources, crop phenology, and crop production modeling difficult.

The objectives of this study include: (1) develop a robust T_s model using limited surface climate variables by integrating soil moisture estimates dynamically as well as snow depth observations; (2) demonstrate the error to contributions in soil temperature modeling; and (3) evaluate the performance of an improved model to predict T_s compared to current models. The datasets and methods used are described in section 2. Section 3 provides modeling results and conclusions are presented in section 4.

2 Datasets and Methods

2.1 Weather stations and datasets

The spatial domain of this study covers the winter wheat belt in the U.S. Great Plains, comprising the states of Nebraska (NE), Kansas (KS), Oklahoma (OK), and part of Texas (TX) where soil texture and bulk density vary (Fig. 1). In this study, three surface climate datasets were obtained from the Automated Weather Data Networks (AWDN) (<https://hprcc.unl.edu/awdn/>), commissioned in the 1980s



for Nebraska and Kansas. The Oklahoma Mesonet is a daily climate data source for Oklahoma, which
115 started in the 1990s (<http://www.mesonet.org/>). For Texas, we selected the Soil and Climate Analysis
Network for its daily climate observations (<https://www.wcc.nrcs.usda.gov/scan/>) due to limited quality
data available in its automated weather station network. The selected stations included 26 in NE, 8 in
KS, 44 in OK, and 9 in TX. The selection of these 87 stations was based on the completeness of climate
120 station datasets, soil datasets providing soil attributes and characteristics were obtained from the
standard USDA-NRCS Soil Survey Geographic (gSSURGO) Database product
(<https://gdg.sc.egov.usda.gov/>), in which soil bulk density (ρ_b , g cm⁻³), soil organic matter (f_{OM} , %),
sand (f_{sa} , %), clay (f_{cl} , %), silt (f_{sl} , %) contents, soil porosity (\emptyset , %), and soil surface albedo (α , -) were
used for all weather stations. Note that all symbols and corresponding descriptions for variables used in
125 this study are listed in the Table A1 (see the Appendix). The snow depth data were taken from the daily
Global Historical Climatology Network (GHCN) (Menne et al., 2009; Lin et al., 2017). Detailed dataset
sources and data variables used in each dataset are shown in Table A2 (see the Appendix).

2.2 Soil temperature models

130 2.2.1 Empirical model

There are two common soil temperature models: empirical and process-based. After examining both
types of models for our study region, the current empirical model was selected because it was more
accurate than the process-based model in this area. Plauborg (2002) developed a statistical soil
temperature (T_s , °C) model based on the current and previous two-day air temperatures (T_a , °C), annual



135 and semi-annual cycles in the soil temperature fluctuations, and a daily soil temperature offset at a specific site, as shown in Eq. (1) (called EM02, thereafter):

$$T_{s,j} = \gamma + \alpha_0 T_{a,j} + \alpha_1 T_{a,j-1} + \alpha_2 T_{a,j-2} + \beta_1 \sin(\omega j) + \delta_1 \cos(\omega j) + \beta_2 \sin(2\omega j) + \delta_2 \cos(2\omega j) \quad (1)$$

where γ is an offset constant ($^{\circ}\text{C}$) and coefficients α_0 , α_1 , and α_2 are dimensionless. The units of the
 140 coefficients β_1 , β_2 , δ_1 , and δ_2 are Celsius ($^{\circ}\text{C}$). The j and ω denote day of the year and annual frequency ($2\pi/365$ or $2\pi/366$ in leap years) in an annual soil temperature signal.

2.2.2 Improved empirical model

The improved model, based on the EM02, was developed through the following three steps: (1)
 145 prolonging the time window of T_a to include one extra prior day T_a ; (2) constructing a new fictive environmental temperature (T_{env} , $^{\circ}\text{C}$) defined as a function of air temperature and surface skin temperature (T_{sfc} , $^{\circ}\text{C}$) (Williams et al., 1984) utilizing T_{env} to replace the original T_a ; and most importantly (3), incorporating site-specific daily soil thermal diffusivity and snow depth (Fig. 2). This improved empirical model (iEM02) can be described by Eqs. (2-6):

$$150 \quad T_{s,j} = (\gamma + \alpha_0 T_{env,j} + \alpha_1 T_{env,j-1} + \alpha_2 T_{env,j-2} + \alpha_3 T_{env,j-3} + \beta_1 \sin(\omega j) + \delta_1 \cos(\omega j) + \beta_2 \sin(2\omega j) + \delta_2 \cos(2\omega j)) \times f(D_{s,j}) \times DR_{eff,j} \quad (2)$$

$$T_{env,j} = \beta T_{a,j} + (1 - \beta) T_{sfc,j} \quad (3)$$

$$T_{sfc,j} = (1 - \alpha) \left(\bar{T}_{a,j} + (\bar{T}_{max,j} - \bar{T}_{a,j}) \sqrt{\frac{R_{s,j}}{33.5}} \right) + \alpha T_{sfc,j-1} \quad (4)$$

$$f(D_{s,j}) = \exp(-f_s D_{s,j}) \quad (5)$$



$$155 \quad DR_{eff,j} = \exp \left(k_0 \sqrt{-h \frac{\pi}{k_{s,j} p}} \right) \quad (6)$$

where β refers to the weighting coefficient for air temperature T_a (-). The T_{sfc} in Eq. (3) was estimated iteratively from the three-day running average of daily air temperature (\bar{T}_a), daily maximum temperature (\bar{T}_{max} , °C), and daily solar radiation (R_s , MJ m⁻² d⁻¹). The α denotes soil surface albedo (-) and initial $T_{sfc,j-1}$ was set as annual mean T_a in Eq. (4). The constant 33.5 is an empirical constant (MJ m⁻² d⁻¹) (Williams et al., 1984). The function of snow cover on the j^{th} day is given as $f(D_{s,j})$ and was introduced based on the work of Rankinen et al., (2004). The f_s and D_s are empirical soil heat damping parameters (m⁻¹) and snow depth (m). The damping ratio of soil at the soil depth of h ($h = 0.1$ m in this study) is $DR_{eff,j}$ (Rosenberg et al., 1983). The weighting coefficient for the damping ratio (-) is k_0 . The p represents the period (365 days or 366 days in a leap year) in an annual cycle. The thermal diffusivity $k_{s,j}$ (m² s⁻¹) is equivalent to thermal conductivity (λ , W m⁻¹ K⁻¹) divided by volumetric heat capacity (C , J m⁻³ K⁻¹) and reflects both the ability of soil to transfer heat and to change temperature when the heat is supplied or dissipated. The estimate of thermal conductivity (λ) and volumetric heat capacity (C) can be described by Eqs. (7-11) (Lu et al., 2014):

$$\lambda_j = \lambda_{dry} + \exp(b_1 - \theta_j^{-b_2}) \quad (7)$$

$$170 \quad \lambda_{dry} = -0.56\theta + 0.51 \quad (8)$$

$$b_1 = 1.97f_{sa} + 1.87\rho_b - 1.36f_{sa}\rho_b - 0.95 \quad (9)$$

$$b_2 = 0.67f_{cl} + 0.24 \quad (10)$$

$$C_j = 1.92 \times 10^6 f_m + 2.51 \times 10^6 f_{OM} + 4.18 \times 10^6 \theta_j \quad (11)$$



where λ_{dry} is oven-dried soil thermal conductivity derived from a linear function of soil porosity (\emptyset , %).

175 Both b_1 and b_2 are the shape factors of the λ curve that are estimated by soil texture components. Soil water content is defined as θ_j on the j^{th} day ($\text{cm}^3 \text{cm}^{-3}$) and was calculated by the soil water balance model (Chalhoub et al., 2017). Briefly, the iEM02 operates on a daily time step as daily soil moisture is a function of soil moisture storage capacity (θ^* , mm), 24-hour precipitation (P , mm), and Penman-Monteith reference evapotranspiration (ET_0 , mm) and are estimated by Eqs. (12-15):

$$180 \quad \theta_r = 0.026 + 0.005f_{cl} + 0.0158f_{OM} \quad (12)$$

$$\beta_{d,j} = 1 - \exp\left(-\frac{6.68\theta_j h}{(\theta_s - \theta_r)h}\right) \quad (13)$$

$$E_j = \begin{cases} P_j + \beta_{d,j}(ET_{0,j} - P_j) & P_j < ET_{0,j} \\ ET_{0,j} & P_j \geq ET_{0,j} \end{cases} \quad (14)$$

$$\theta_j h = \begin{cases} \theta_r h & \theta_j h \leq \theta_r h \\ \theta_{j-1} h + (P_{j-1} - E_{j-1}) & \theta_r h < \theta_j h < \theta^* h \\ \theta_s h & \theta_j h \geq \theta^* h \end{cases} \quad (15)$$

where θ_r and θ_s define residual and saturated volumetric soil water contents ($\text{cm}^3 \text{cm}^{-3}$). θ_s is assumed to
 185 be equal to soil porosity while $\beta_{d,j}$ is a weighting coefficient for the difference between ET_0 (Allen et al., 1998) and P on the j^{th} day (-). The initial soil water content (θ_{j-1}) is assumed to be equal half of soil porosity.

Climate observation data prior to the year 2015 were selected to calibrate the iEM02 for each station.
 190 For NE, KS, and OK, daily soil temperature observations at each station had at least 10 years in daily time series for calibrations. Datasets from TX had at least 4 years available for calibrations. Climate variables used for calibration included air temperature, precipitation, snow depth, and solar radiation



daily observations and the site's static soil property. The optimal parameter values for each weather station were estimated when a minimum root mean square (RMSE) between estimated and observed soil temperature was achieved. These parameters for all 87 stations are listed in Table A3 (see the Appendix).

2.3 iEM02 evaluation

In the datasets selected, all 87 station observations were longer than 15 years except for stations located in Texas. The last five-year observations (2015 to 2019) were used to independently conduct model validation for all 87 stations. The metrics used to evaluate model performance were root mean square error (RMSE) and mean absolute error (MAE). Soil temperature modeling improvement was evaluated by relative RMSE changes $\left[-\frac{100(RMSE_{improved} - RMSE_{original})}{RMSE_{original}} \right]$ and by intercomparison between the fully complete model and the reduced model.

205

3 Results and discussion

3.1 Improved empirical model (iEM02)

The iEM02 was evaluated from 2015 to 2019 for 87 weather stations. Soil temperature modeling using different soil textures was improved in different ways in the iEM02 model (Fig. 3). The improvement of soil temperature modeling improvement by relative RMSE changes was different for different sites. The weather stations located in NE and KS as well as TX showed less improvement by introducing the air temperature of $T_{a,j-3}$ compared to OK (Fig. 3a). The soil types in OK are more clay and silt compared to NE and KS (Fig. 1). However, the improvement by using the fictive environmental temperature was

210



significant in northern areas of NE and KS but not in the southern area of OK and part of TX (Fig. 3b).

215 Overall, latitude-dominated air temperature should play a role in improving estimated soil temperature. Most of the 87 stations achieved a 15% to 40% improvement in simulated soil temperature by introducing air temperature $T_{a,j-3}$ and replacing T_a with T_{env} . This improvement was in agreement with a previous study (Dolschak et al., 2015). By incorporating changes in soil moisture and daily snow depth, additional improvements in soil temperature simulation of up to 50% could be achieved (Fig. 3c)

220 compared to the original model EM02. It should be noted that there were fewer stations available in KS and TX compared to NE and OK. Overall, integrating snow cover and soil moisture data in iEM02 improved the simulated soil temperature (Fig. 3).

3.2 iEM02's parameters

225 The parameters described in iEM02 for each weather station are indicative of soil temperature sensitivities for each independent variable in Eq. (2) although strictly speaking, they are not mathematical sensitivities (Fig. 4 & Table A2). For T_{env} , the current day T_{env} was the most weighted as expected (Fig. 4a). The parameters of T_{env} for the prior day 1 to day 3 were relatively weak in terms of absolute magnitudes due to autoregression properties in the soil temperature (Figs. 4b-d). Interestingly,

230 in the iEM02 model, the prior day 2 was negatively associated with soil temperature (Fig. 4c) which cannot be interpreted by soil physical processes but in a more autoregressive sense in which the soil temperature signals are superimposed. The periodic property embedded in iEM02 was two low-frequency components (semi-annual and annual signals). Obviously, the annual signal strength indicated by β_1 and δ_1 was one-order stronger than the semi-annual signal strengths in soil temperature



235 (Fig. 4e-h). The result also suggested the strong β_1 and δ_1 spatial contexts of the northern region (e.g., in Nebraska and Kansas) were differently weighted than those from the southern region (e.g., in Oklahoma and Texas). For the snow damping factor, the snow cover had a larger impact on soil temperature in the northern region when compared to the southern region (Fig. 4i). However, the soil damping ratio factor was relatively evenly distributed (Fig. 4j).

240 RMSE performance is shown in Figure 5 when the iEM02 was a complete model vs. the reduced model iEM02 where one independent variable term was removed. When removing any one independent variable, the modeled soil temperature RMSE increased from 110% to 130% (Fig. 5), indicating a 20% drop in RMSE if one independent variable was removed in the iEM02 model. Specifically, the iEM02 model performance decreased (i.e., RMSE increased from 0.1 to 0.4°C) when the α_0 term was removed
245 (Fig. 5, a-d). Unlike α_0 , removing the β_1 term was not as sensitive and gave an increase of 0.1-0.2°C RMSE on average for all states in the region (Fig. 5, e-h). However, it is clear that the iEM02 model was most sensitive to δ_1 . With the removal of δ_1 from the complete iEM02 model, the RMSE increased 0.3-0.4°C for all four states (Fig. 5, i-l). Due to the location-dependency of the above coefficients, further spatial interpolation of the iEM02 model would be beneficial to predict soil temperature for
250 irrigated agricultural areas without weather stations in the U.S. Great Plains and to improve water and crop management modeling.

3.3 Spatial and temporal modeling performance

A graphical summary of how closely the modeled soil temperature agreed with the observed soil
255 temperature for each weather station is shown in Figure 6. Daily T_s estimated in the iEM02 model



outperformed that in the original EM02 model for all 87 weather stations. For example, both mean absolute error (MAE) and root mean square error (RMSE) were decreased on average by 0.6°C when the iEM02 model was used to estimate T_s . Individually, the improved model showed a less than 1.6°C RMSE for any individual station but 16% of the stations had larger than 2°C RMSE in the original
260 EM02. In addition, we compared the performance of iEM02 against a recent energy-balance model (Chalhoub et al., 2017). Our prediction of T_s was improved by 1.2°C RMSE compared to the energy-balance model (not shown).

Spatial distributions of RMSE showed that the majority of weather stations had better performance in
265 Oklahoma with a mean RMSE of 1.9 and 1.1°C for EM02 and iEM02, respectively, whereas Nebraska had a RMSE of 2.1 and 1.3°C for EM02 and iEM02, respectively. The different modeling performance was associated with the soil heat transport process and how frequent snowfall could be observed in Nebraska and Oklahoma. Similar results were presented in a recent study by (Huang et al., 2017). On the other hand, the high quality of weather data from the Oklahoma Mesonet considered to be the "gold
270 standard" for the statewide weather network (Lin et al., 2016) thus ensured quality of both model calibrations and observed soil temperature in Oklahoma.

Seasonal T_s indicated that iEM02 modeling was mostly improved in the spring season from 2°C to 1.3°C RMSE (Fig. 7a) but the original model EM02 showed the uncertainty was in good agreement
275 with the performance achieved in Plauborg (2002). All other seasons were improved in similar ways from 1.8°C to 1.2 or 1.3°C RMSE. The improvement for all seasons could be attributed to introducing



soil diffusivity, which changed with daily soil moisture and snow cover, and this affected the soil thermal conductivity (Rankinen et al., 2004; Zhang, 2005). Moreover, although modeling wintertime soil temperature improved from 1.8°C to 1.3°C RMSE, which was the same as in the summer (Fig. 7),
280 the soil temperature located in more frequent snow-covered states, (e.g., Nebraska and Kansas), was better improved when T_{env} and snow depth were introduced (Rankinen et al., 2004; Dutta et al., 2018).

Since precipitation gradients exist in the U.S. Great Plains from western to eastern regions (Evetts et al., 2020), three subregions were classified for each state as western (100°W towards west), central
285 (between 97° and 100°W), and eastern (97°W towards east). Figure 8 displays the time series of EM02 modeled, iEM02 modeled, and observed soil temperatures only covering winter wheat growing seasons (October 1 to June 30) for four growing seasons from 2015 to 2019 (validation periods) in Nebraska and Kansas. All subregions in Nebraska and Kansas showed improvement when using the iEM02 model (Fig. 8). Similarly, the iEM02 improved the RMSE during four growing seasons in Oklahoma and
290 Texas (Fig. 9). The EM02 model had the best performance in Oklahoma with a mean RMSE of 1.0°C, while the mean RMSE in Kansas was 1.4°C in EM02. Soil temperatures estimated by iEM02 had approximately a 0.3 to 0.4°C RMSE (Figs. 8 and 9). In addition, larger improvements by iEM02 were observed in most subregions during wintertime, which would be beneficial for modeling accurately winter wheat yields and potential yields (Persson et al., 2017).

295

4. Conclusion



The primary intention of this work was to develop an improved soil temperature model for the U.S. Great Plains that can predict soil temperature by using common weather station variables as inputs. The improved empirical model (iEM02) integrated soil thermal diffusivity and snow cover factors, and they significantly improved the estimate of soil temperature for 87 weather stations in the U.S. Great Plains that were studied. Specifically, after incorporating changes in soil moisture and daily snow depth, the improved model showed a near 50% gain in performance in terms of RMSE decrease in the improved model compared to the original model. The value of RMSE across 87 stations was 0.6°C lower on average than the original model from 2015 to 2019. We concluded that the iEM02 model can estimate better soil temperature at the surface soil layer where most hydrological and biological processes occur. Both seasonal and spatial improvements made in the improved model demonstrated the robustness of the iEM02 model, suggesting this improved model can provide a reliable simulation of soil temperature to use in modeling hydrological process and crop production in the U.S. Great Plains.



310 Appendix

Table A1. Table of symbols and corresponding descriptions used in this paper.

Symbols	Descriptions	Units
α	soil surface albedo	(-)
$\alpha_0, \alpha_1, \alpha_2, \alpha_3$	empirical parameters of air temperature to estimate soil temperature	(-)
β	empirical parameter of air temperature to calculate environmental temperature	(-)
β_1, β_2	empirical parameters of sine wave to estimate soil temperature	(°C)
β_d	empirical parameter of evapotranspiration for actual evapotranspiration	(-)
δ_1, δ_2	empirical parameters of cosine wave to estimate soil temperature	(°C)
γ	offset constant	(°C)
λ	soil thermal conductivity	(W m ⁻¹ K ⁻¹)
λ_{dry}	oven-dried soil thermal conductivity	(W m ⁻¹ K ⁻¹)
\emptyset	soil porosity	(%)
ω	annual frequency ($2\pi/365$ or $2\pi/366$ in any leap years)	(-)
$\theta, \theta_r, \theta_s$	actual, residual, and saturated soil water content	(m ³ m ⁻³)
ρ_b	soil bulk density	(g cm ⁻³)
b_1, b_2	shape factors of soil thermal conductivity curve	(-)
C	soil volumetric heat capacity	(J m ⁻³ K ⁻¹)
D_s	snow depth	(m)
DR_{eff}	effective soil damping ratio	(-)
E, ET_0	actual and reference evapotranspiration	(mm)
$f_{cl}, f_m, f_{OM}, f_{sa}$	clay, mineral, organic matter, and sand content in the soil profile	(%)
f_s	empirical parameters of snow depth	(m ⁻¹)
h	soil depth	(m)
j	day of year	(day)
k_0	empirical parameter of soil damping ratio	(-)
k_s	soil thermal diffusivity	(m ² s ⁻¹)
p	period of year (365 days or 366 days in any leap year)	days
P	precipitation	mm
R_s	solar radiation	(MJ m ⁻² d ⁻¹)
T_a, T_{max}	mean and maximum air temperature at 2 m height	(°C)
T_{env}	fictive environmental temperature	(°C)
T_s	bared soil temperature at 0.1 m depth	(°C)
T_{sfc}	surface skin temperature	(°C)
RMSE, MAE	root mean square error and mean absolute error	(°C)



Table A2. List of datasets used in this study including the data source (Networks), state names
 315 (Coverage States), and specific data variables (Variables). Data sources include the Gridded Soil Survey
 Geographic (gSSURGO), the Automated Weather Data Network – High Plains Regional Climate
 Center (AWDN), the Oklahoma Mesonet (OK Mesonet), the Soil Climate Analysis Network (SCAN),
 and the daily Global History Climatology Network (dGHCN). Weather stations from four states were
 located in the U.S. Great Plains including Nebraska (NE), Kansas (KS), Oklahoma (OK), and Texas
 320 (TX). Climate data reports daily maximum (T_{max} , °C) and minimum air temperature (T_{min} , °C) at 2 m
 height, relative humidity (RH , %), rainfall ($prcp$, mm), solar radiation (R_s , MJ m⁻² day⁻¹), wind speed at
 2 m (WS , m s⁻¹), and snow depth (D_s , mm). Soil data consists of the daily bare soil temperature at 10 cm
 depth (T_s , °C), albedo of soil surface (α , -), organic matter content (f_{OM} , %), bulk density (ρ_b , g cm⁻³),
 porosity (\emptyset , %), sand (f_{sa}), silt (f_{sl}), and clay (f_{cl}) content (%).

Networks	Coverage States	Variables
gSSURGO	NE, KS, OK, TX	$\alpha, f_{OM}, \rho_b, \emptyset, f_{sa}, f_{sl},$ and f_{cl}
AWDN	NE and KS	$T_{max}, T_{min}, RH, prcp, R_s, WS,$ and T_s
OK Mesonet	OK	$T_{max}, T_{min}, RH, prcp, R_s, WS,$ and T_s
SCAN	TX	$T_{max}, T_{min}, RH, prcp, R_s, WS,$ and T_s
dGHCN	NE, KS, OK, TX	D_s

325



330 **Table A3.** List of model parameters for each weather station in the U.S. Great Plains. The location consists of latitude (Lat) and longitude (Lon). There are 12 parameters in the improved EM model including parameters of air temperature (β , -); parameters for current day to previous three-day of T_{env} : α_0 (-), α_1 (-), α_2 (-), α_3 (-), and constant offset γ (°C); annual and semi-annual waves of sine and cosine functions parameters: β_1 , β_2 , δ_1 , δ_2 (°C); parameters for snow depth damping factor (f_s , m⁻¹) and the soil damping factor (k_0 , -). The bold font indicates that estimated coefficients are not statistically significant at 95% confidence intervals.

Location		Parameters in iEM02											
Lat	Lon	β	α_0	α_1	α_2	α_3	γ	β_1	δ_1	β_2	δ_2	f_s	k_0
26.52	-98.06	0.2	0.402	0.132	-0.18	0.237	7.684	-0.895	-2.212	-0.233	-0.171	-0.05	-0.001
29.33	-103.2	0.3	0.517	0.162	-0.22	0.174	6.221	-0.717	-3.852	0.037	-0.398	-0.106	-0.001
30.27	-97.74	0.8	0.247	0.191	0.017	0.1	8.416	-1.373	-3.454	0.03	-0.269	-0.079	-0.001
31.62	-102.8	0.3	0.369	0.193	-0.13	0.165	6.647	-1.195	-4.451	0.127	-0.365	0.093	-0.001
32.75	-97	0.8	0.216	0.217	0.015	0.088	9.768	-1.338	-2.746	-0.048	-0.167	0.001	0.002
33.59	-102.4	0.3	0.359	0.186	-0.161	0.163	5.656	-1.153	-4.435	0.335	-0.314	0.696	-0.064
33.63	-102.8	0.1	0.421	0.087	-0.175	0.228	4.153	-1.366	-4.637	0.201	-0.077	-0.27	-0.047
33.89	-97.27	0.7	0.415	0.196	-0.01	0.054	4.712	-0.732	-4.197	0.18	0.019	1.187	-0.034
33.96	-102.8	0.3	0.411	0.14	-0.13	0.134	4.949	-1.002	-4.61	0.456	-0.256	0.695	0.001
34.03	-95.54	0.8	0.535	0.136	-0.003	0.058	4.076	-1.164	-2.726	0.306	0.065	-2.045	-0.049
34.04	-96.94	0.6	0.475	0.143	-0.054	0.064	5.196	-1.152	-4.172	0.199	0.054	2.23	-0.066
34.17	-97.99	0.7	0.39	0.103	-0.02	0.056	5.867	-1.032	-3.753	0.136	-0.173	0.232	-0.156
34.19	-97.59	0.8	0.407	0.099	0.009	0.043	4.471	-0.809	-3.197	0.085	-0.091	-1.257	-0.194
34.22	-95.25	0.8	0.408	0.154	0.018	0.049	5.564	-1.358	-3.863	0.104	0.168	-4.133	-0.053
34.31	-96	0.8	0.476	0.097	0.001	0.048	5.499	-1.161	-3.493	0.06	0.015	0.133	-0.108
34.31	-94.82	0.9	0.408	0.139	0.025	0.062	5.947	-0.934	-3.235	0.066	0.006	6.601	-0.065

335



Location		Parameters in iEM02											
lat	lon	β	α_0	α_1	α_2	α_3	γ	β_1	δ_1	β_2	δ_2	f_s	k_0
34.57	-96.95	0.5	0.451	0.142	-0.083	0.091	6.331	-1.225	-4.095	0.016	0.075	-1.584	-0.079
34.59	-99.34	0.9	0.266	0.158	0.032	0.071	6.781	-1.68	-4.029	0.345	-0.198	3.081	-0.094
34.61	-96.33	0.5	0.502	0.176	-0.081	0.099	4.733	-1.073	-4.454	0.103	-0.234	-4.241	-0.015
34.66	-95.33	0.9	0.466	0.165	0.021	0.06	5.079	-0.917	-3.484	0.13	0.183	-14.03	-0.029
34.69	-99.83	0.7	0.49	0.153	-0.029	0.056	5.682	-1.341	-4.035	0.139	0.121	-0.068	-0.048
34.73	-98.57	0.9	0.338	0.134	0.019	0.055	4.763	-1.015	-3.158	0.18	0.003	1.937	-0.179
34.8	-96.67	0.7	0.454	0.105	-0.02	0.065	5.742	-1.185	-3.628	0.088	-0.056	-1.26	-0.102
34.81	-98.02	0.8	0.328	0.138	0.008	0.053	5.727	-1.1	-3.811	0.124	-0.05	0.761	-0.129
34.88	-95.78	0.8	0.404	0.111	0.005	0.052	4.723	-1.099	-3.134	0.179	0.018	-0.012	-0.2
35.03	-97.91	0.7	0.52	0.141	-0.028	0.052	5.008	-1.008	-3.33	0.136	0.163	0.845	-0.065
35.19	-102.1	0.6	0.239	0.139	-0.014	0.088	5.715	-1.807	-4.526	0.267	-0.208	-0.129	-0.131
35.27	-97.96	0.8	0.381	0.176	0.011	0.055	5.053	-1.161	-3.341	0.22	-0.093	-0.502	-0.101
35.51	-98.78	0.8	0.39	0.17	0.006	0.05	3.781	-0.779	-2.908	0.078	-0.321	4.582	-0.16
35.55	-99.73	0.5	0.533	0.124	-0.09	0.116	4.372	-1.198	-3.711	0.291	-0.041	0.086	-0.062
35.58	-95.91	0.7	0.391	0.152	-0.015	0.05	5.284	-1.013	-4.053	0.128	0.114	1.057	-0.113
35.59	-99.27	0.8	0.467	0.136	0.011	0.056	5.461	-1.244	-3.594	0.182	0.143	1.237	-0.042
35.68	-94.85	0.6	0.446	0.148	-0.049	0.076	4.758	-1.353	-4.102	0.187	0.248	-3.491	-0.059
35.84	-96	0.6	0.341	0.178	-0.026	0.097	6.618	-1.783	-4.72	0.358	-0.191	-1.872	-0.023
35.85	-97.48	0.9	0.333	0.174	0.021	0.066	5.67	-1.493	-3.899	0.143	0.083	0.914	-0.092
35.97	-94.99	0.7	0.45	0.136	-0.016	0.05	5.637	-1.502	-3.517	0.233	0.094	0.225	-0.047
36	-97.05	0.7	0.414	0.114	-0.007	0.038	4.93	-0.909	-3.849	0.154	-0.037	3.355	-0.156
36.03	-96.5	0.7	0.385	0.149	-0.012	0.053	5.87	-1.13	-4.099	0.093	-0.006	2.131	-0.088
36.07	-99.9	0.7	0.354	0.176	-0.002	0.055	5.608	-1.196	-4.61	0.169	-0.252	1.315	-0.075
36.12	-97.1	0.7	0.377	0.172	-0.009	0.056	5.897	-1.314	-4.027	0.162	0.031	2.05	-0.062
36.26	-98.5	0.7	0.429	0.15	-0.021	0.055	4.908	-1.27	-4.183	0.25	0.265	0.169	-0.067
36.41	-97.69	0.6	0.397	0.175	-0.038	0.079	5.029	-1.188	-4.643	0.089	-0.276	1.137	-0.062
36.42	-96.04	0.9	0.36	0.144	0.017	0.048	5.533	-1.159	-3.882	0.118	0.069	3.667	-0.104
36.52	-96.34	0.7	0.308	0.157	-0.005	0.063	5.684	-1.494	-4.43	0.29	0.149	0.563	-0.13
36.6	-101.6	0.7	0.453	0.173	-0.015	0.078	5.052	-1.21	-3.919	0.261	-0.057	1.796	-0.03
36.63	-96.81	0.6	0.545	0.151	-0.08	0.067	4.993	-0.829	-3.553	0.061	0.031	0.66	-0.061
36.69	-102.5	0.7	0.223	0.16	0.008	0.057	5.711	-1.795	-5.263	0.235	-0.155	1.458	-0.125
36.75	-98.36	0.5	0.474	0.152	-0.083	0.082	4.968	-1.198	-4.11	0.191	-0.011	3.696	-0.072
36.75	-97.25	0.7	0.383	0.167	-0.02	0.056	5.197	-1.086	-4.062	0.005	0.001	4.13	-0.083
36.83	-99.64	0.7	0.354	0.189	-0.004	0.074	5.242	-1.28	-4.03	0.204	0.047	0.367	-0.054
36.84	-96.43	0.6	0.382	0.209	-0.028	0.066	5.279	-1.386	-4.9	0.418	-0.258	-7.259	-0.014
36.9	-96.91	0.6	0.374	0.16	-0.031	0.06	5.007	-1.266	-4.123	0.152	0.021	4.473	-0.103
36.91	-95.89	0.6	0.415	0.169	-0.045	0.053	5.844	-1.22	-4.352	0.235	-0.255	6.361	-0.063
37.37	-95.3	0.7	0.373	0.173	-0.016	0.076	4.535	-1.64	-4.396	0.047	-0.009	-0.77	-0.021



Location		Parameters in iEM02											
lat	lon	β	α_0	α_1	α_2	α_3	γ	β_1	δ_1	β_2	δ_2	f_S	k_0
37.98	-100.8	0.7	0.346	0.185	0.001	0.077	4.153	-1.319	-4.886	0.084	-0.441	1.602	-0.074
38.45	-101.8	0.4	0.297	0.142	-0.073	0.124	5.091	-2.004	-6.426	0.18	-0.585	1.573	-0.038
38.53	-95.25	0.6	0.46	0.176	-0.053	0.071	3.971	-1.302	-3.761	0.128	-0.075	1.529	-0.054
39.07	-95.78	0.6	0.387	0.162	-0.033	0.089	4.229	-1.715	-4.991	0.019	0.126	0.279	-0.048
39.2	-96.6	0.5	0.4	0.163	-0.077	0.107	4.461	-1.724	-4.951	-0.021	0.081	1.77	-0.025
39.38	-101.1	1	0.252	0.188	0.055	0.075	4.641	-1.501	-5.624	0.062	-0.369	1.507	-0.078
39.82	-97.85	0.8	0.437	0.182	0.008	0.058	3.385	-1.482	-4.33	-0.004	-0.109	-0.429	-0.068
40.08	-98.28	0.5	0.44	0.151	-0.076	0.076	4.164	-1.339	-4.958	-0.017	-0.093	7.636	-0.046
40.3	-96.93	0.7	0.381	0.205	-0.014	0.072	3.293	-1.615	-4.407	0.204	0.088	0.342	-0.064
40.32	-99.38	0.6	0.319	0.199	-0.027	0.055	4.414	-1.593	-5.523	0.25	-0.063	6.898	-0.1
40.4	-101.7	0.6	0.364	0.145	-0.031	0.079	3.559	-1.151	-5.266	0.402	-0.162	8.794	-0.12
40.5	-99.37	0.6	0.337	0.202	-0.029	0.08	4.765	-1.676	-5.194	0.307	0.153	2.688	-0.029
40.52	-99.05	0.6	0.379	0.172	-0.031	0.068	3.676	-1.45	-4.852	0.281	-0.026	5.941	-0.086
40.57	-99.7	0.5	0.329	0.18	-0.051	0.085	3.856	-1.901	-5.549	0.302	0.214	9.566	-0.085
40.57	-98.15	0.8	0.28	0.158	0.013	0.056	4.244	-1.671	-4.596	0.205	0.072	0.708	-0.245
40.63	-100.5	0.7	0.36	0.199	-0.015	0.064	3.888	-1.484	-5.794	0.089	-0.136	3.376	-0.054
40.72	-99.02	0.6	0.406	0.195	-0.034	0.076	3.572	-1.456	-5.1	0.205	0.043	0.756	-0.032
40.75	-98.77	0.5	0.437	0.158	-0.075	0.081	3.778	-1.502	-5.411	0.35	0.097	2.179	-0.078
40.82	-96.67	0.6	0.384	0.193	-0.048	0.066	4.302	-1.619	-4.854	0.111	0.079	3.63	-0.102
40.85	-96.62	0.2	0.588	0.032	-0.209	0.173	3.744	-1.616	-4.753	0.141	0.275	11.447	-0.048
40.86	-98.47	0.5	0.521	0.151	-0.089	0.074	2.731	-1.53	-4.791	0.114	0.309	7.99	-0.067
41.15	-96.5	0.7	0.354	0.169	-0.011	0.065	4.615	-1.819	-4.679	0.124	0.05	4.403	-0.07
41.15	-96.42	0.6	0.42	0.172	-0.055	0.071	3.925	-1.883	-5.022	0.105	0.102	3.669	-0.053
41.22	-103	0.7	0.323	0.188	-0.001	0.054	3.392	-1.118	-5.154	0.263	-0.119	10.875	-0.072
41.4	-97.53	0.5	0.489	0.131	-0.082	0.082	3.624	-1.5	-4.763	0.389	0.074	5.878	-0.057
41.62	-98.95	0.6	0.403	0.164	-0.039	0.077	3.52	-1.649	-5.573	0.136	0.093	2.696	-0.074
41.85	-96.75	0.7	0.336	0.201	-0.025	0.076	4.125	-1.82	-5.053	0.296	0.099	11.111	-0.057
41.88	-103.7	0.7	0.346	0.2	-0.007	0.07	3.58	-1.41	-5.435	0.44	-0.079	4.335	-0.061
41.9	-100.2	0.3	0.548	0.125	-0.195	0.144	2.915	-1.653	-4.817	0.187	0.146	1.078	-0.043
41.93	-98.2	0.5	0.417	0.159	-0.073	0.074	3.353	-1.279	-4.421	0.243	-0.076	10.447	-0.078
42.47	-98.77	0.5	0.509	0.13	-0.104	0.091	3.542	-1.505	-4.489	0.129	0.231	2.505	-0.056
42.57	-99.83	0.3	0.54	0.074	-0.182	0.156	3.049	-1.454	-5.465	0.202	0.286	1.976	-0.077
42.75	-102.2	0.7	0.43	0.144	-0.024	0.068	2.82	-1.142	-5.151	0.141	0.249	3.492	-0.089



Code availability

MATLAB code is available upon request.

340

Data availability

Data used in this study are available by the links above (material and methods).

Author contribution

345 HD and XL designed the experiments, conducted simulations, analyzed the data, and wrote the manuscript. NW helped data analysis, result interpretation, and discussion. MBK and GFS provided suggestions and discussion, wrote and revised the manuscript.

Competing interests

350 The authors declare that they have no conflict of interest.

Acknowledgements

This study was supported in part by the U.S. Department of Agriculture (ARS grant no. 58-3090-5-009 and NIFA grant no. 2016-68007- 25066) and the Kansas Crop Improvement Association, the U.S.
355 Department of Agriculture National Institute of Food and Agriculture, Hatch project 1018005. The contribution number of this manuscript is 21-250-J. We appreciated Dr. Gerard Kluitenberg and Dr. Jesse Tack at Kansas State University for providing helpful suggestions to improve the quality of paper. We thank Dallas Staley for her outstanding contribution in editing and finalizing the paper. Her work continues to be at the highest professional level.

360



References

- Abu-Hamdeh, N. H.: Thermal Properties of Soils as affected by Density and Water Content, *Biosystems Engineering*, 86, 97-102, 10.1016/s1537-5110(03)00112-0, 2003.
- 400 Allen, R. G., Pereira, L. S., Raes, D., and Smith, M.: Crop evapotranspiration-Guidelines for computing crop water requirements-FAO Irrigation and drainage paper 56, Fao, Rome, 300, D05109, 1998.
- Araghi, A., Mousavi-Baygi, M., Adamowski, J., Martinez, C., and van der Ploeg, M.: Forecasting soil temperature based on surface air temperature using a wavelet artificial neural network, *Meteorological Applications*, 24, 603-611, 10.1002/met.1661, 2017.
- 405 Badache, M., Eslami-Nejad, P., Ouzzane, M., Aidoun, Z., and Lamarche, L.: A new modeling approach for improved ground temperature profile determination, *Renewable Energy*, 85, 436-444, 10.1016/j.renene.2015.06.020, 2016.
- Badía, D., López-García, S., Martí, C., Ortíz-Perpiñá, O., Girona-García, A., and Casanova-Gascón, J.: Burn effects on soil properties associated to heat transfer under contrasting moisture content, *Science of the Total Environment*, 601, 1119-1128, 2017.
- 410 Bergjord, A. K., Bonesmo, H., and Skjelvåg, A. O.: Modelling the course of frost tolerance in winter wheat, *European Journal of Agronomy*, 28, 321-330, 10.1016/j.eja.2007.10.002, 2008.
- Bittelli, M., Ventura, F., Campbell, G. S., Snyder, R. L., Gallegati, F., and Pisa, P. R.: Coupling of heat, water vapor, and liquid water fluxes to compute evaporation in bare soils, *Journal of Hydrology*, 362, 191-205, 10.1016/j.jhydrol.2008.08.014, 2008.
- 415 Brock, F. V. and Crawford, K. C.: The Oklahoma Mesonet_ A Technical Overview, *Journal of Atmospheric and Oceanic Technology*, 1995.
- Chalhoub, M., Bernier, M., Coquet, Y., and Philippe, M.: A simple heat and moisture transfer model to predict ground temperature for shallow ground heat exchangers, *Renewable Energy*, 103, 295-307, 10.1016/j.renene.2016.11.027, 2017.
- 420 Dirmeyer, P. A. and Norton, H. E.: Indications of surface and sub-surface hydrologic properties from SMAP soil moisture retrievals, *Hydrology*, 5, 36, 2018.
- Dolschak, K., Gartner, K., and Berger, T. W.: A new approach to predict soil temperature under vegetated surfaces, *Modeling earth systems and environment*, 1, 32, 2015.
- Dutta, B., Grant, B. B., Congreves, K. A., Smith, W. N., Wagner-Riddle, C., VanderZaag, A. C., Tenuta, M., and Desjardins, R. L.: Characterising effects of management practices, snow cover, and soil texture on soil temperature: Model development in DNDC, *Biosystems Engineering*, 168, 54-72, 10.1016/j.biosystemseng.2017.02.001, 2018.
- 425 Evett, S. R., Colaizzi, P. D., Lamm, F. R., O'Shaughnessy, S. A., Heeren, D. M., Trout, T. J., Kranz, W. L., and Lin, X.: Past, present, and future of irrigation on the US Great Plains, *Transactions of the ASABE*, 63, 703-729, 2020.
- Goulden, M., Wofsy, S., Harden, J., Trumbore, S. E., Crill, P., Gower, S., Fries, T., Daube, B., Fan, S.-M., and Sutton, D.: Sensitivity of boreal forest carbon balance to soil thaw, *Science*, 279, 214-217, 1998.
- 430 Gupta, S. C., Radke, J. K., Swan, J. B., and Moncrief, J. F.: Predicting soil temperature under a ridge-furrow system in the U.S. Corn Belt, *Soil & Tillage Research*, 18, 145-165, 1990.
- Haacker, E. M., Cotterman, K. A., Smidt, S. J., Kendall, A. D., and Hyndman, D. W.: Effects of management areas, drought, and commodity prices on groundwater decline patterns across the High Plains Aquifer, *Agricultural Water Management*, 218, 259-273, 2019.
- 435 Hillel, D.: *Environmental soil physics: Fundamentals, applications, and environmental considerations*, Elsevier 1998.
- Huang, Y., Jiang, J., Ma, S., Ricciuto, D., Hanson, P. J., and Luo, Y.: Soil thermal dynamics, snow cover, and frozen depth under five temperature treatments in an ombrotrophic bog: Constrained forecast with data assimilation, *Journal of Geophysical Research: Biogeosciences*, 122, 2046-2063, 10.1002/2016jg003725, 2017.
- 440 Kang, S., Kim, S., Oh, S., and Lee, D.: Predicting spatial and temporal patterns of soil temperature based on topography, surface cover and air temperature, *Forest Ecology and Management*, 136, 173-184, 2000.
- Lakshmi, V., Jackson, T. J., and Zehrhuhs, D.: Soil moisture-temperature relationships: results from two field experiments, *Hydrological processes*, 17, 3041-3057, 2003.
- Lembrechts, J. J., Aalto, J., Ashcroft, M. B., De Frenne, P., Kopecky, M., Lenoir, J., Luoto, M., Maclean, I. M. D., Roupsard, O., Fuentes-Lillo, E., Garcia, R. A., Pellissier, L., Pitteloud, C., Alatalo, J. M., Smith, S. W., Bjork, R. G., Muffler, L., Ratier Backes, A., Cesarz, S., Gottschall, F., Okello, J., Urban, J., Plichta, R., Svatek, M., Phartyal, S. S.,



- 450 Wipf, S., Eisenhauer, N., Puskas, M., Turtureanu, P. D., Varlagin, A., Dimarco, R. D., Jump, A. S., Randall, K.,
Dorrepaal, E., Larson, K., Walz, J., Vitale, L., Svoboda, M., Finger Higgens, R., Halbritter, A. H., Curasi, S. R., Klupar,
I., Koontz, A., Pearse, W. D., Simpson, E., Stenkovski, M., Jessen Graae, B., Vedel Sorensen, M., Hoye, T. T.,
Fernandez Calzado, M. R., Lorite, J., Carbognani, M., Tomaselli, M., Forte, T. G. W., Petraglia, A., Haesen, S., Somers,
455 B., Van Meerbeek, K., Bjorkman, M. P., Hylander, K., Merinero, S., Gharun, M., Buchmann, N., Dolezal, J., Matula, R.,
Thomas, A. D., Bailey, J. J., Ghosn, D., Kazakis, G., de Pablo, M. A., Kemppinen, J., Niittynen, P., Rew, L., Seipel, T.,
Larson, C., Speed, J. D. M., Ardo, J., Cannone, N., Guglielmin, M., Malfasi, F., Bader, M. Y., Canessa, R., Stanisci, A.,
Kreyling, J., Schmeddes, J., Teuber, L., Aschero, V., Ciliak, M., Malis, F., De Smedt, P., Govaert, S., Meeussen, C.,
Vangansbeke, P., Gigauri, K., Lamprecht, A., Pauli, H., Steinbauer, K., Winkler, M., Ueyama, M., Nunez, M. A., Ursu,
460 T. M., Haider, S., Wedegartner, R. E. M., Smiljanic, M., Trouillier, M., Wilmking, M., Altman, J., Bruna, J., Hederova,
L., Macek, M., Man, M., Wild, J., Vittoz, P., Partel, M., Barancok, P., Kanka, R., Kollar, J., Palaj, A., Barros, A.,
Mazzolari, A. C., Bauters, M., Boeckx, P., Benito Alonso, J. L., Zong, S., Di Cecco, V., Sitkova, Z., Tielborger, K., van
den Brink, L., Weigel, R., Homeier, J., Dahlberg, C. J., Medinets, S., Medinets, V., De Boeck, H. J., Portillo-Estrada, M.,
Verryckt, L. T., Milbau, A., Daskalova, G. N., Thomas, H. J. D., Myers-Smith, I. H., Blonder, B., Stephan, J. G.,
465 Descombes, P., Zellweger, F., Frei, E. R., Heinesch, B., Andrews, C., Dick, J., Siebicke, L., Rocha, A., Senior, R. A.,
Rixen, C., Jimenez, J. J., Boike, J., Pauchard, A., Scholten, T., Scheffers, B., Klinges, D., Basham, E. W., Zhang, J.,
Zhang, Z., Geron, C., Fazlioglu, F., Candan, O., Sallo Bravo, J., Hrbacek, F., Laska, K., Cremonese, E., Haase, P.,
Moyano, F. E., Rossi, C., and Nijs, I.: SoilTemp: A global database of near-surface temperature, *Glob Chang Biol*,
10.1111/gcb.15123, 2020.
- 465 Liang, L. L., Riveros-Iregui, D. A., Emanuel, R. E., and McGlynn, B. L.: A simple framework to estimate distributed soil
temperature from discrete air temperature measurements in data-scarce regions, *Journal of Geophysical Research:*
Atmospheres, 119, 407-417, 10.1002/2013jd020597, 2014.
- Lin, X., Pielke Sr, R. A., Mahmood, R., Fiebrich, C. A., and Aiken, R.: Observational evidence of temperature trends at two
levels in the surface layer, *Atmospheric Chemistry and Physics*, 16, 827-841, 10.5194/acp-16-827-2016, 2016.
- 470 Lin, X., Harrington, J., Ciampitti, I., Gowda, P., Brown, D., and Kisekka, I.: Kansas trends and changes in temperature,
precipitation, drought, and frost-free days from the 1890s to 2015, *Journal of Contemporary Water Research &
Education*, 162, 18-30, 2017.
- Lu, Y., Lu, S., Horton, R., and Ren, T.: An Empirical Model for Estimating Soil Thermal Conductivity from Texture, Water
Content, and Bulk Density, *Soil Science Society of America Journal*, 78, 1859-1868, 10.2136/sssaj2014.05.0218, 2014.
- 475 Menne, M. J., Williams Jr, C. N., and Vose, R. S.: The US Historical Climatology Network monthly temperature data,
version 2, *Bulletin of the American Meteorological Society*, 90, 993-1008, 2009.
- Meyer, N., Welp, G., and Amelung, W.: The temperature sensitivity (Q10) of soil respiration: controlling factors and spatial
prediction at regional scale based on environmental soil classes, *Global Biogeochemical Cycles*, 32, 306-323, 2018.
- 480 Mihalakakou, G., Santamouris, M., Lewis, J., and Asimakopoulos, D.: On the application of the energy balance equation to
predict ground temperature profiles, *Solar Energy*, 60, 181-190, 1997.
- Miller, K., Luck, J., Heeren, D. M., Lo, T., Martin, D., and Barker, J.: A geospatial variable rate irrigation control scenario
evaluation methodology based on mining root zone available water capacity, *Precision agriculture*, 19, 666-683, 2018.
- Nagare, R. M., Schincariol, R. A., Quinton, W. L., and Hayashi, M.: Effects of freezing on soil temperature, freezing front
propagation and moisture redistribution in peat: laboratory investigations, *Hydrology and Earth System Sciences*, 16,
485 501-515, 2012.
- Nobel, P. S. and Geller, G. N.: Temperature modelling of wet and dry desert soils, *The Journal of Ecology*, 247-258, 1987.
- Onwuka, B. and Mang, B.: Effects of soil temperature on some soil properties and plant growth, *Adv. Plants Agric. Res*, 8,
34-37, 2018.
- Paulsen, G. M. and Heyne, E. G.: Grain production of winter wheat after spring freeze injury, *Agronomy Journal*, 75, 1983.
- 490 Persson, T. and Wirén, A.: Nitrogen mineralization and potential nitrification at different depths in acid forest soils, in:
Nutrient uptake and cycling in forest ecosystems, Springer, 55-65, 1995.
- Persson, T., Bergjord Olsen, A. K., Nkurunziza, L., Sindhøj, E., and Eckersten, H.: Estimation of Crown Temperature of
Winter Wheat and the Effect on Simulation of Frost Tolerance, *Journal of Agronomy and Crop Science*, 203, 161-176,
10.1111/jac.12187, 2017.



- 495 Plauborg, F.: Simple model for 10 cm soil temperature in different soils with short grass, *European Journal of Agronomy*, 17, 173-179, 2002.
- Qi, J., Zhang, X., and Cosh, M. H.: Modeling soil temperature in a temperate region: A comparison between empirical and physically based methods in SWAT, *Ecological Engineering*, 129, 134-143, 2019.
- 500 Qi, J., Li, S., Li, Q., Xing, Z., Bourque, C. P.-A., and Meng, F.-R.: A new soil-temperature module for SWAT application in regions with seasonal snow cover, *Journal of Hydrology*, 538, 863-877, 2016.
- Rankinen, K., Karvonen, T., and Butterfield, D.: A simple model for predicting soil temperature in snow-covered and seasonally frozen soil: model description and testing, *Hydrology and Earth System Sciences*, 8, 706-716, 10.5194/hess-8-706-2004, 2004.
- Rosenberg, N. J., Blad, B. L., and Verma, S. B.: *Microclimate: the biological environment*, John Wiley & Sons 1983.
- 505 Smith, K. A.: *Soil and environmental analysis: physical methods, revised, and expanded*, CRC Press 2000.
- Soong, J. L., Phillips, C. L., Ledna, C., Koven, C. D., and Torn, M. S.: CMIP5 models predict rapid and deep soil warming over the 21st century, *Journal of Geophysical Research: Biogeosciences*, 125, e2019JG005266, 2020.
- Stone, P., Sorensen, I., and Jamieson, P.: Effect of soil temperature on phenology, canopy development, biomass and yield of maize in a cool-temperate climate, *Field crops research*, 63, 169-178, 1999.
- 510 Tack, J., Barkley, A., and Nalley, L. L.: Effect of warming temperatures on US wheat yields, *Proc Natl Acad Sci U S A*, 112, 6931-6936, 10.1073/pnas.1415181112, 2015.
- Williams, J., Jones, C., and Dyke, P. T.: A modeling approach to determining the relationship between erosion and soil productivity, *Transactions of the ASAE*, 27, 129-0144, 1984.
- Williams, J. R., Jones, C. A., Kiniry, J. R., and Spanel, D. A.: The EPIC Crop Growth Model, *Transactions of the American Society of Agricultural Engineers*, 32, 497-511, 1989.
- 515 Wu, S. and Jansson, P.-E.: Modelling soil temperature and moisture and corresponding seasonality of photosynthesis and transpiration in a boreal spruce ecosystem, *Hydrology & Earth System Sciences*, 17, 2013.
- Yan, Q., Duan, Z., Mao, J., Li, X., and Dong, F.: Effects of root-zone temperature and N, P, and K supplies on nutrient uptake of cucumber (*Cucumis sativus* L.) seedlings in hydroponics, *Soil Science and Plant Nutrition*, 58, 707-717, 10.1080/00380768.2012.733925, 2012.
- 520 Yener, D., Ozgener, O., and Ozgener, L.: Prediction of soil temperatures for shallow geothermal applications in Turkey, *Renewable and Sustainable Energy Reviews*, 70, 71-77, 10.1016/j.rser.2016.11.065, 2017.
- Zhang, T.: Influence of the seasonal snow cover on the ground thermal regime: An overview, *Reviews of Geophysics*, 43, 10.1029/2004rg000157, 2005.
- 525 Zhang, T., Shen, S., Cheng, C., Song, C., and Ye, S.: Long-Range Correlation Analysis of Soil Temperature and Moisture on A'rou Hillsides, Babao River Basin, *Journal of Geophysical Research: Atmospheres*, 123, 10.1029/2018jd029094, 2018.
- Zhang, Y., Wang, S., Barr, A. G., and Black, T.: Impact of snow cover on soil temperature and its simulation in a boreal aspen forest, *Cold Regions Science and Technology*, 52, 355-370, 2008.
- 530 Zheng, D., Hunt Jr, E. R., and Running, S. W.: A daily soil temperature model based on air temperature and precipitation for continental applications, *Climate Research*, 2, 183-191, 1993.



Figure Captions (9 Figures)

535 **Figure 1:** Specific soil textures (**a**) and soil bulk density (**b**) at 87 weather stations in the U.S. winter wheat belt including the states of Nebraska (NE), Kansas (KS), Oklahoma (OK), and part of Texas (TX) in the U.S. Great Plains.

Figure 2: Effects of soil moisture on (**a**) thermal conductivity (λ) and (**b**) soil thermal diffusivity (k) obtained by Eqs. (7-11).

540 **Figure 3:** Percentage increments of soil temperature modeling improvement in iEM02 as determined by RMSE changes $\left[-\frac{100(RMSE_{improved} - RMSE_{original})}{RMSE_{original}}\right]$ (**a**) after introducing air temperature of $T_{a,j-3}$, (**b**) after substituting air temperature T_a by fictive environmental temperature (T_{env}), and (**c**) after integrating the impacts of soil thermal diffusivity and snow cover. The colorbar was coded by the improved percentage of iEM02 against the EM02 model.

545 **Figure 4:** Spatial variations of the improved empirical model (iEM) coefficients: (**a-d**) for α_0 , α_1 , α_2 , and α_3 , (**e-h**) for β_1 , δ_1 , β_2 , and δ_2 , (**i**) snow damping ratio (f_s) and (**j**) soil damping ratio coefficients (k_0). The colorbar defines the values of the model's coefficients.

550 **Figure 5:** One-to-one plots of absolute mean errors between the complete model and reduced model in the improved empirical model (iEM02): (**a-d**) with vs. without α_4 in Nebraska (NE), Kansas (KS), Oklahoma (OK), and Texas (TX), respectively, (**e-h**) with vs. without β_1 in Nebraska (NE), Kansas (KS), Oklahoma (OK), and Texas (TX), respectively; (**i-l**) with vs. without δ_1 in NE, KS, OK, and TX, respectively. $RMSE_{reduced}$ and $RMSE_{complete}$ refer to root mean square error for reduced and complete models, respectively. The colorbar indicates the number of observed data points.

555 **Figure 6:** Spatial distribution of mean absolute error (MAE) (a, c) and RMSE (b, d) for an empirical model (EM02, a, b), and improved model iEM02 (iEM02, c, d). The colorbar defines values of MAE ($^{\circ}\text{C}$) and RMSE ($^{\circ}\text{C}$).

Figure 7: Seasonal comparison between estimated and observed soil temperatures: (**a-d**) the empirical model (EM), and (**e-h**) the improved empirical model (iEM02). RMSE was calculated as the root mean square error between estimated and observed soil temperature. "N" refers to the sample size and the gray line represents the 1:1 line. The colorbar describes the number of data points.

560 **Figure 8:** Comparison between observed (grey line), complete model (EM02, green line) and improved model (iEM02, blue line) daily soil temperature in western ($>100^{\circ}\text{W}$), central (between 97° and 100°W), and eastern ($<97^{\circ}\text{W}$) Nebraska (**a-c**) and Kansas (**d-f**) during the winter wheat growing seasons from 2015 to 2019. RMSE is the root mean square error ($^{\circ}\text{C}$). Shaded areas indicate winter season (Dec-Feb).

565 **Figure 9:** The same as Fig. 9 but for western, central, and eastern Oklahoma (**a-c**) and Texas (**d-f**).



Figure 1.

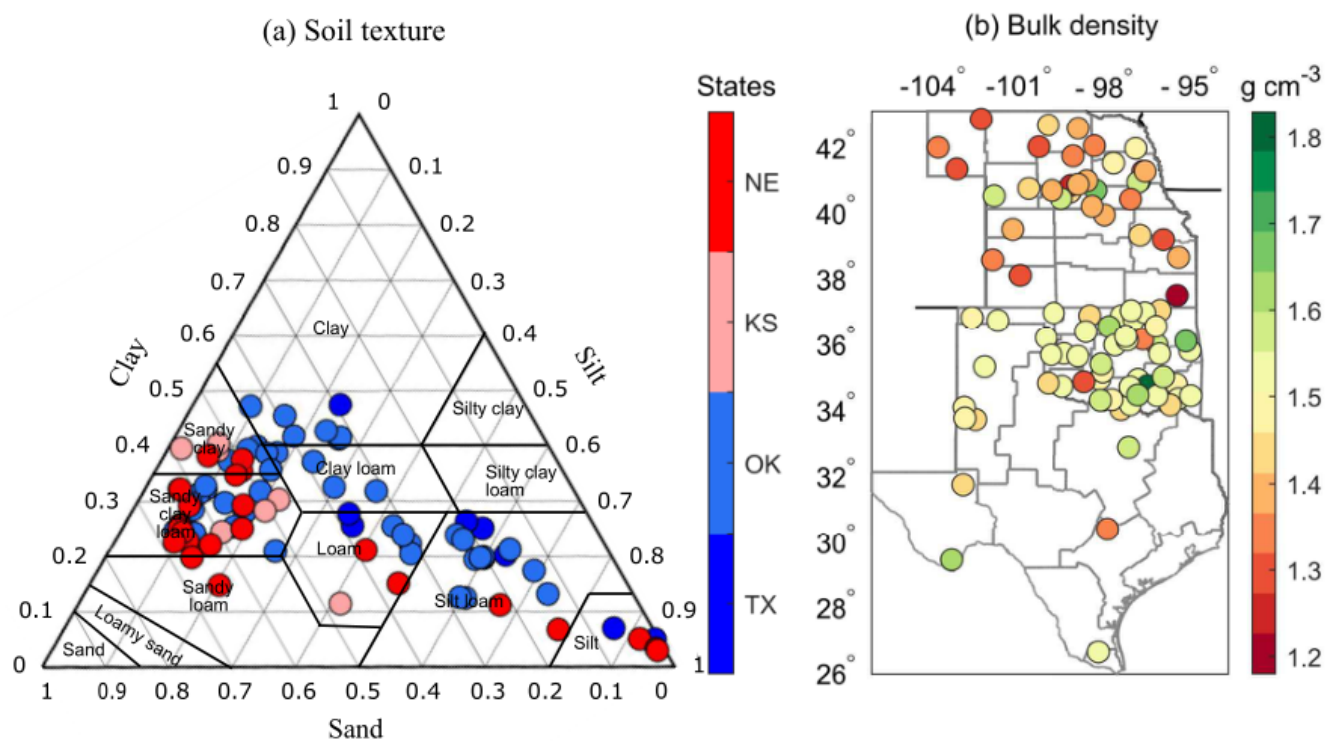


Figure 1: Specific soil textures (a) and soil bulk density (b) at 87 weather stations in the U.S. winter wheat belt including the states of Nebraska (NE), Kansas (KS), Oklahoma (OK), and part of Texas (TX) in the U.S. Great Plains.



Figure 2.

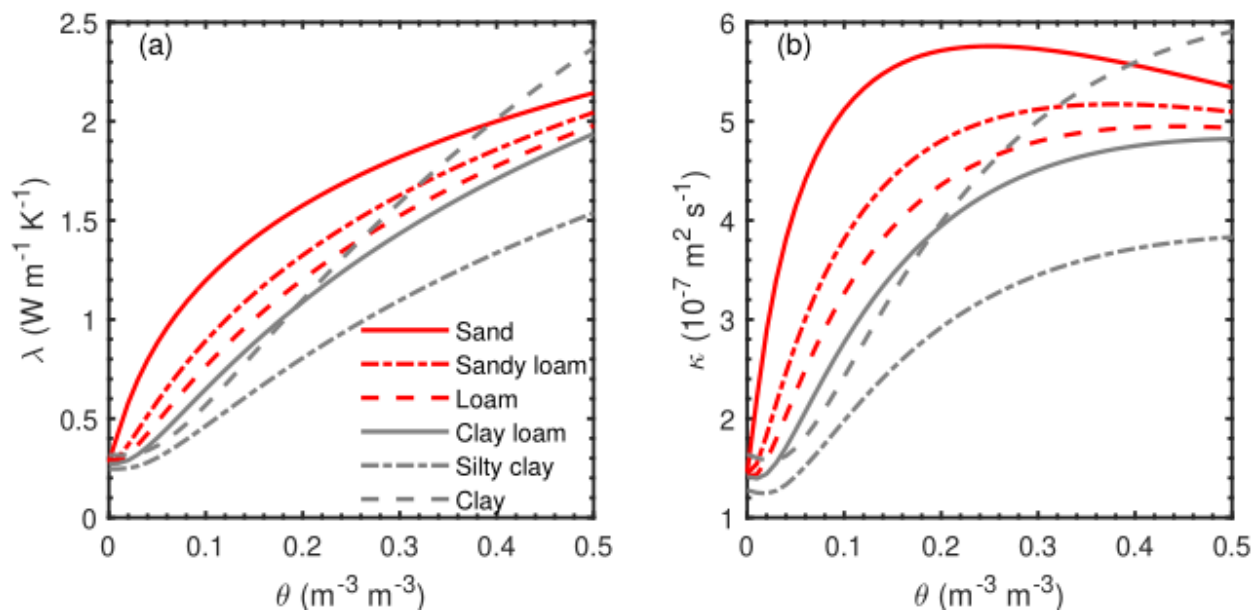


Figure 2: Effects of soil moisture on (a) thermal conductivity (λ) and (b) soil thermal diffusivity (k) obtained by Eqs. (7-11).
575



Figure 3.

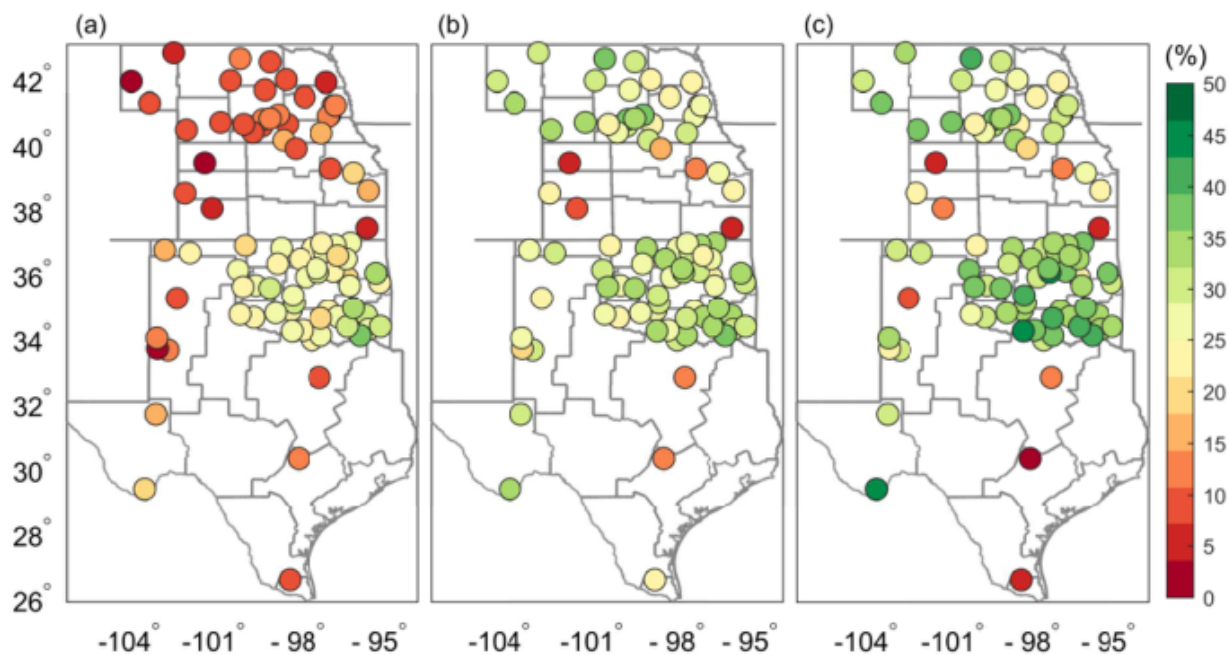


Figure 3: Percentage increments of soil temperature modeling improvement in iEM02 as determined by
 580 RMSE changes $\left[-\frac{100(RMSE_{improved} - RMSE_{original})}{RMSE_{original}} \right]$ (a) after introducing air temperature of $T_{a,j-3}$, (b)
 after substituting air temperature T_a by fictive environmental temperature (T_{env}), and (c) after integrating
 the impacts of soil thermal diffusivity and snow cover. The colorbar was coded by the improved
 percentage of iEM02 against the EM02 model.



585 **Figure 4.**

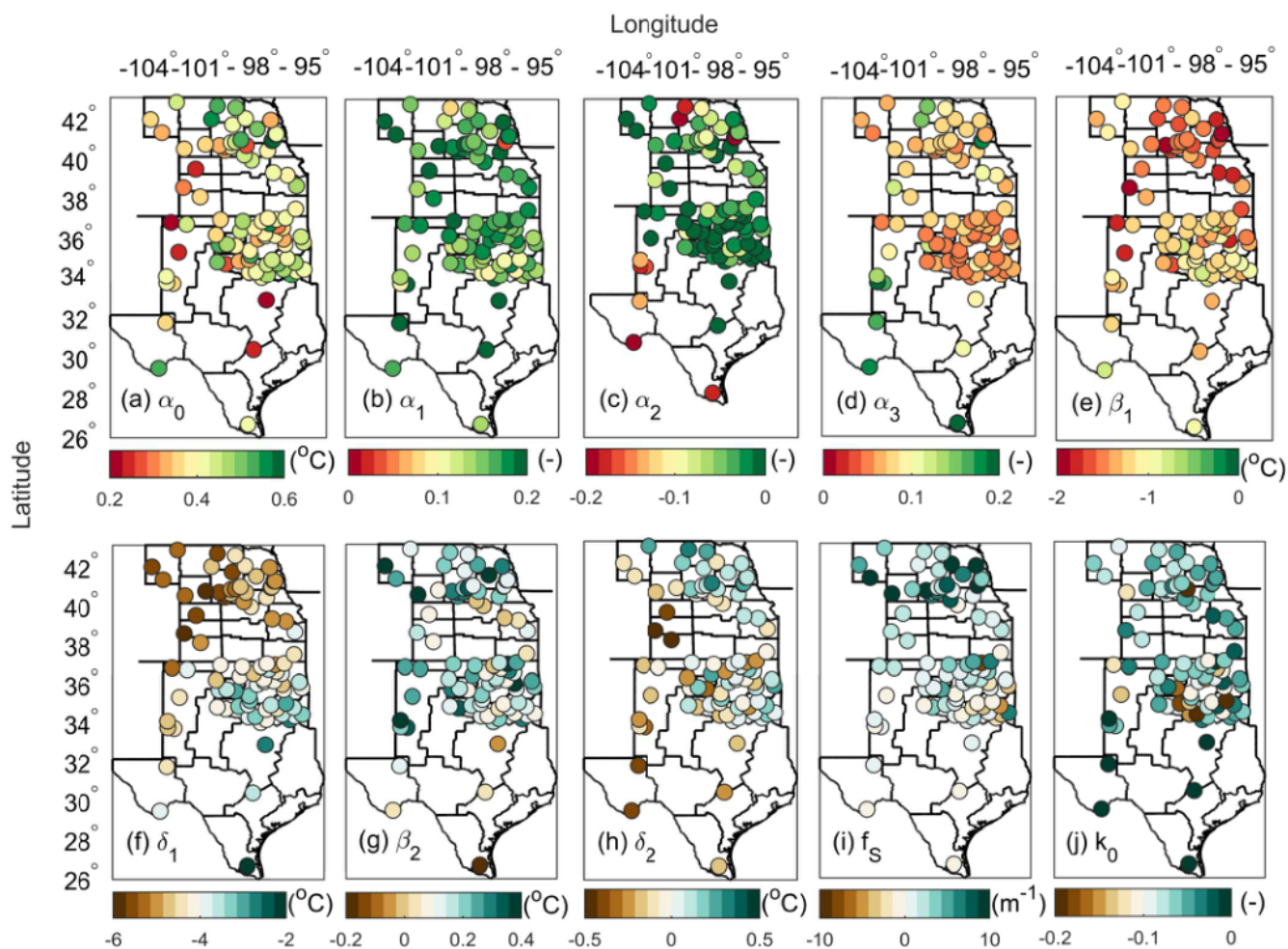


Figure 4: Spatial variations of the improved empirical model (iEM) coefficients: (a-d) for α_0 , α_1 , α_2 , and α_3 , (e-h) for β_1 , δ_1 , β_2 , and δ_2 , (i) snow damping ratio (f_s) and (j) soil damping ratio coefficients (k_0). The colorbar defines the values of the model's coefficients.



Figure 5.

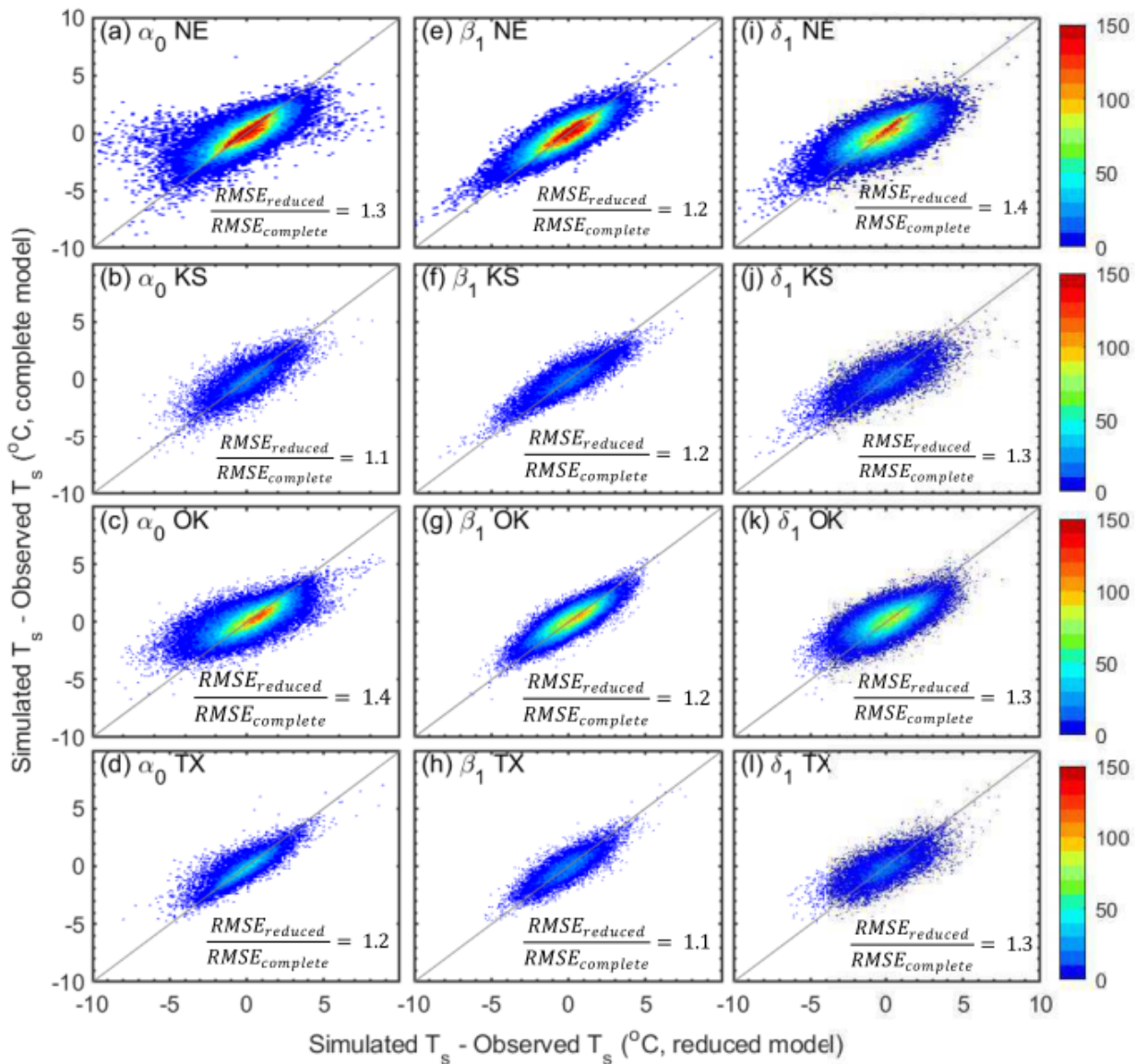
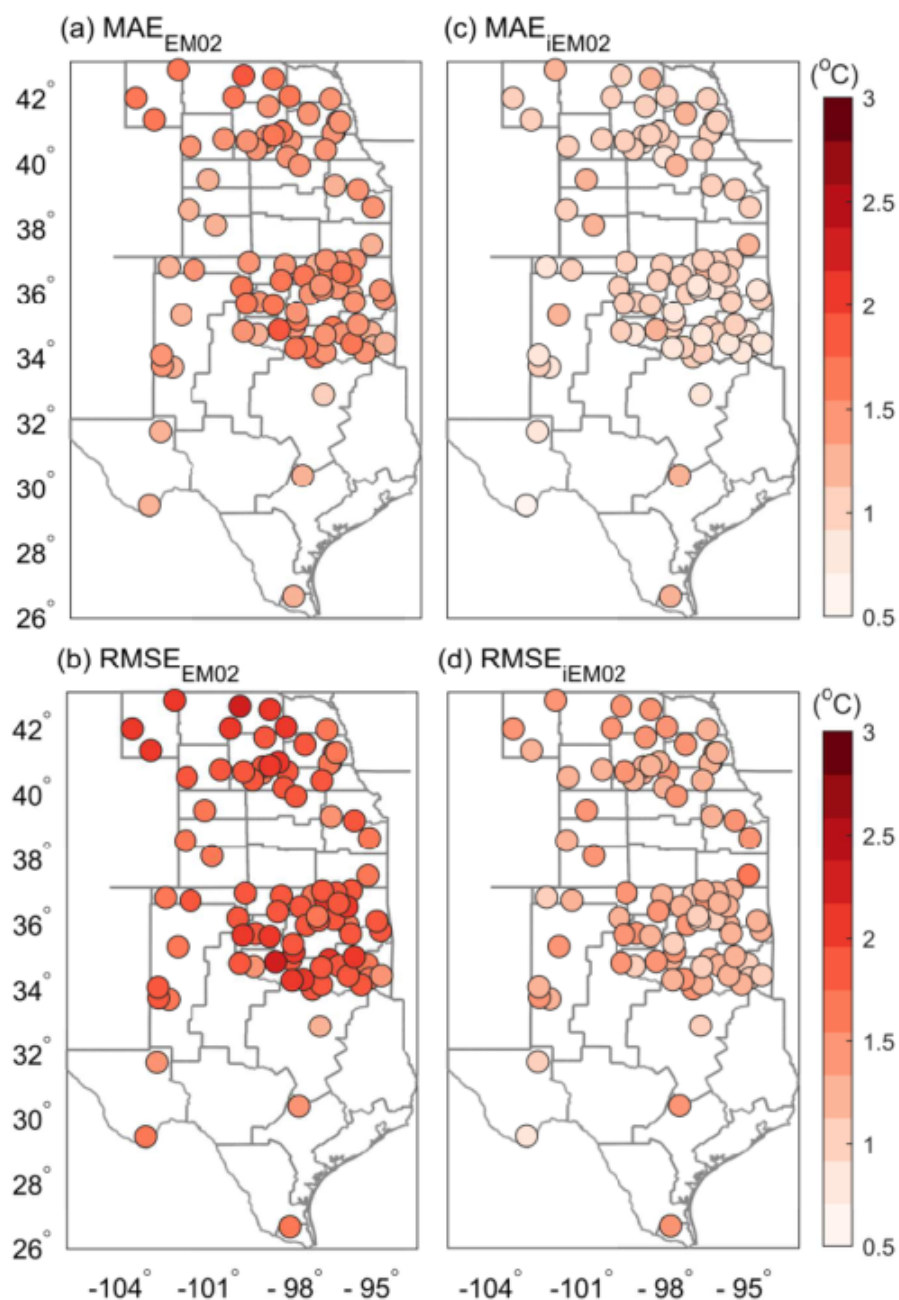


Figure 5: One-to-one plots of absolute mean errors between the complete model and reduced model in the improved empirical model (iEM02): (a-d) with vs. without α_4 in Nebraska (NE), Kansas (KS), Oklahoma (OK), and Texas (TX), respectively, (e-h) with vs. without β_1 in Nebraska (NE), Kansas (KS), Oklahoma (OK), and Texas (TX), respectively; (i-l) with vs. without δ_1 in NE, KS, OK, and TX, respectively. $RMSE_{reduced}$ and $RMSE_{complete}$ refer to root mean square error for reduced and complete models, respectively. The colorbar indicates the number of observed data points.

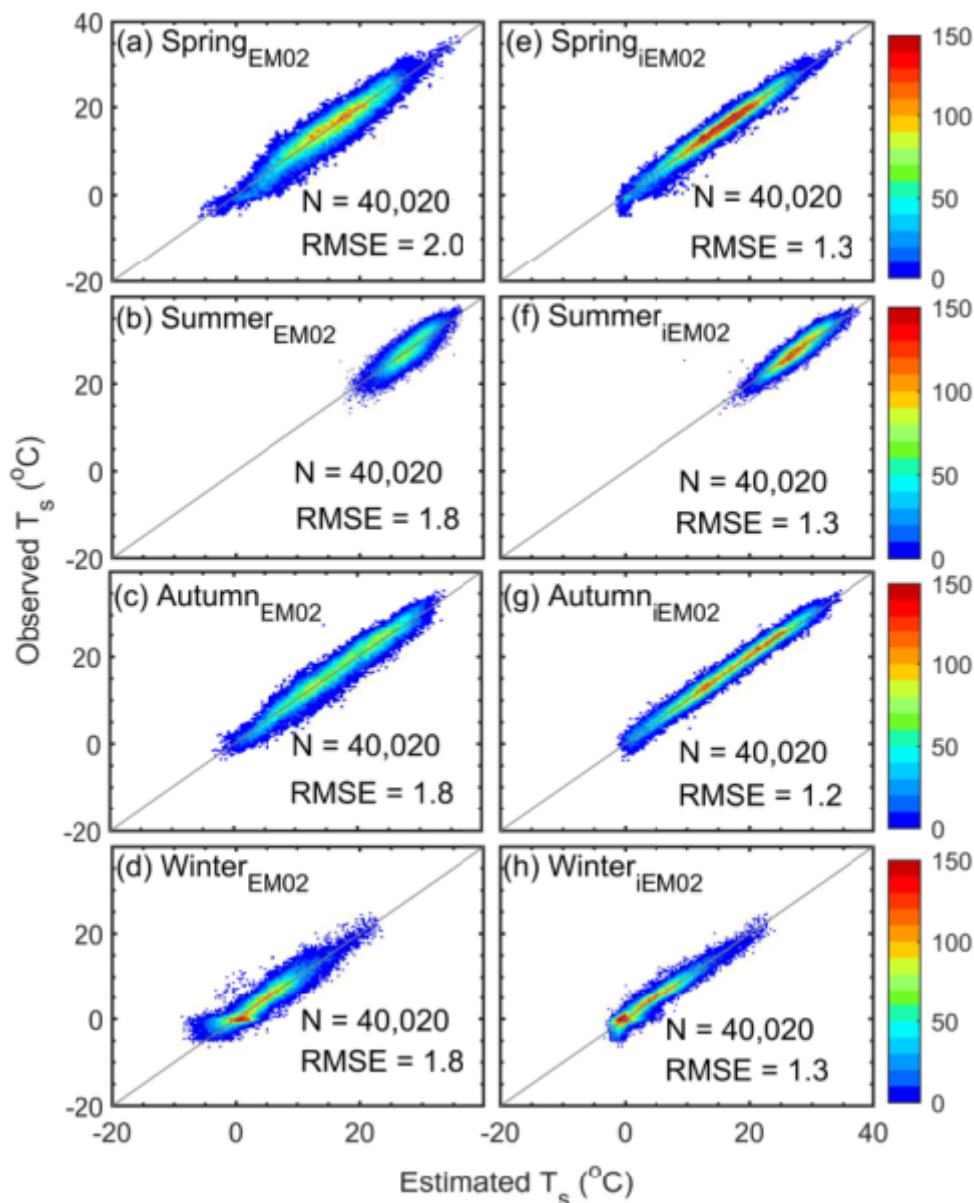
Figure 6.



600

Figure 6: Spatial distribution of mean absolute error (MAE) (a, c) and RMSE (b, d) for an empirical model (EM02, a, b), and improved model iEM02 (iEM02, c, d). The colorbar defines values of MAE ($^{\circ}\text{C}$) and RMSE ($^{\circ}\text{C}$).

Figure 7.



605 **Figure 7:** Seasonal comparison between estimated and observed soil temperatures: (a-d) the empirical model (EM), and (e-h) the improved empirical model (iEM02). RMSE was calculated as the root mean square error between estimated and observed soil temperature. "N" refers to the sample size and the gray line represents the 1:1 line. The colorbar describes the number of data points.



610 **Figure 8.**

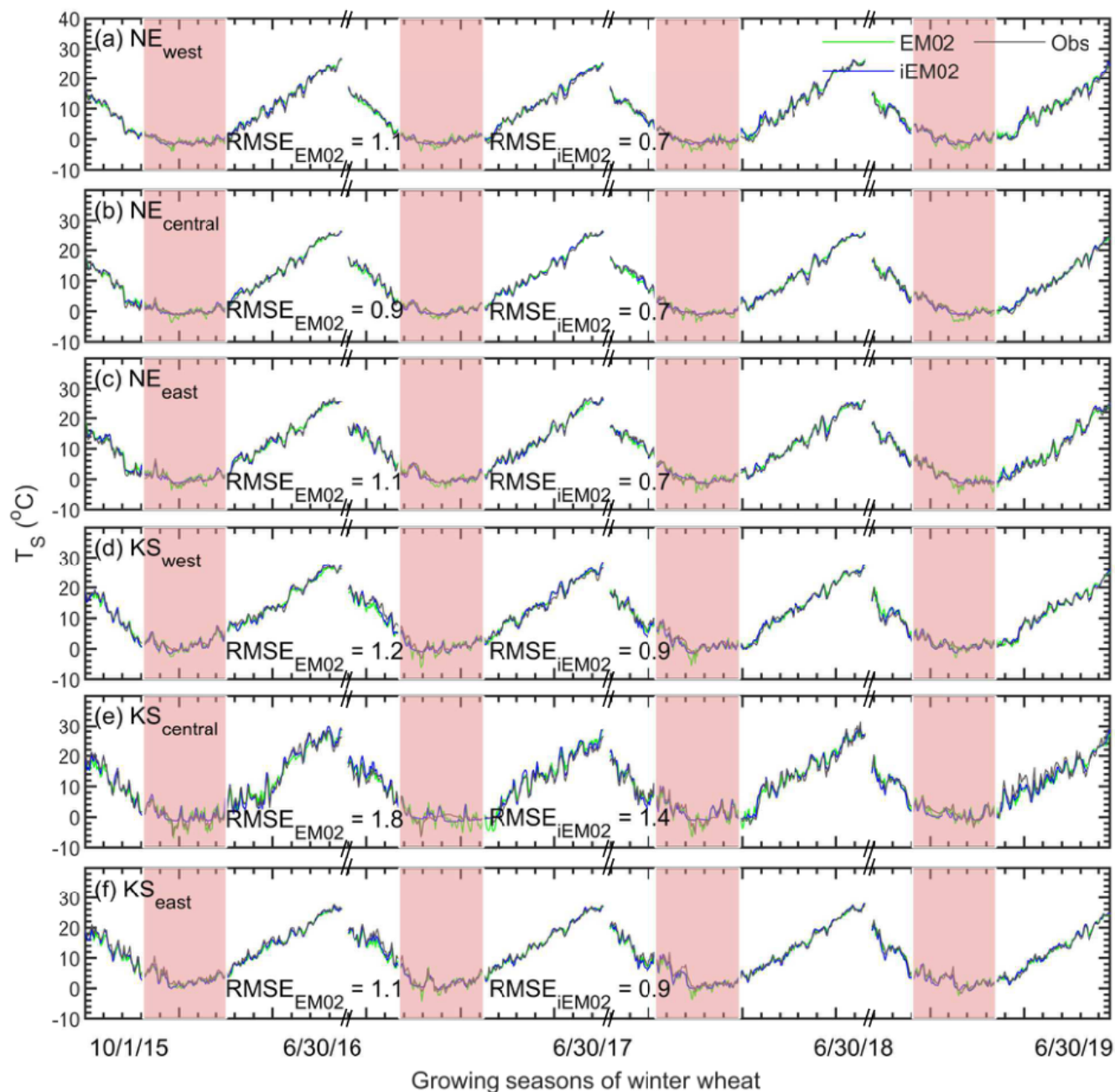


Figure 8: Comparison between observed (grey line), complete model (EM02, green line) and improved model (iEM02, blue line) daily soil temperature in western ($>100^{\circ}\text{W}$), central (between 97° and 100°W), and eastern ($<97^{\circ}\text{W}$) Nebraska (a-c) and Kansas (d-f) during the winter wheat growing seasons from 2015 to 2019. RMSE is the root mean square error ($^{\circ}\text{C}$). Shaded areas indicate winter season (Dec-Feb).

615



Figure 9.

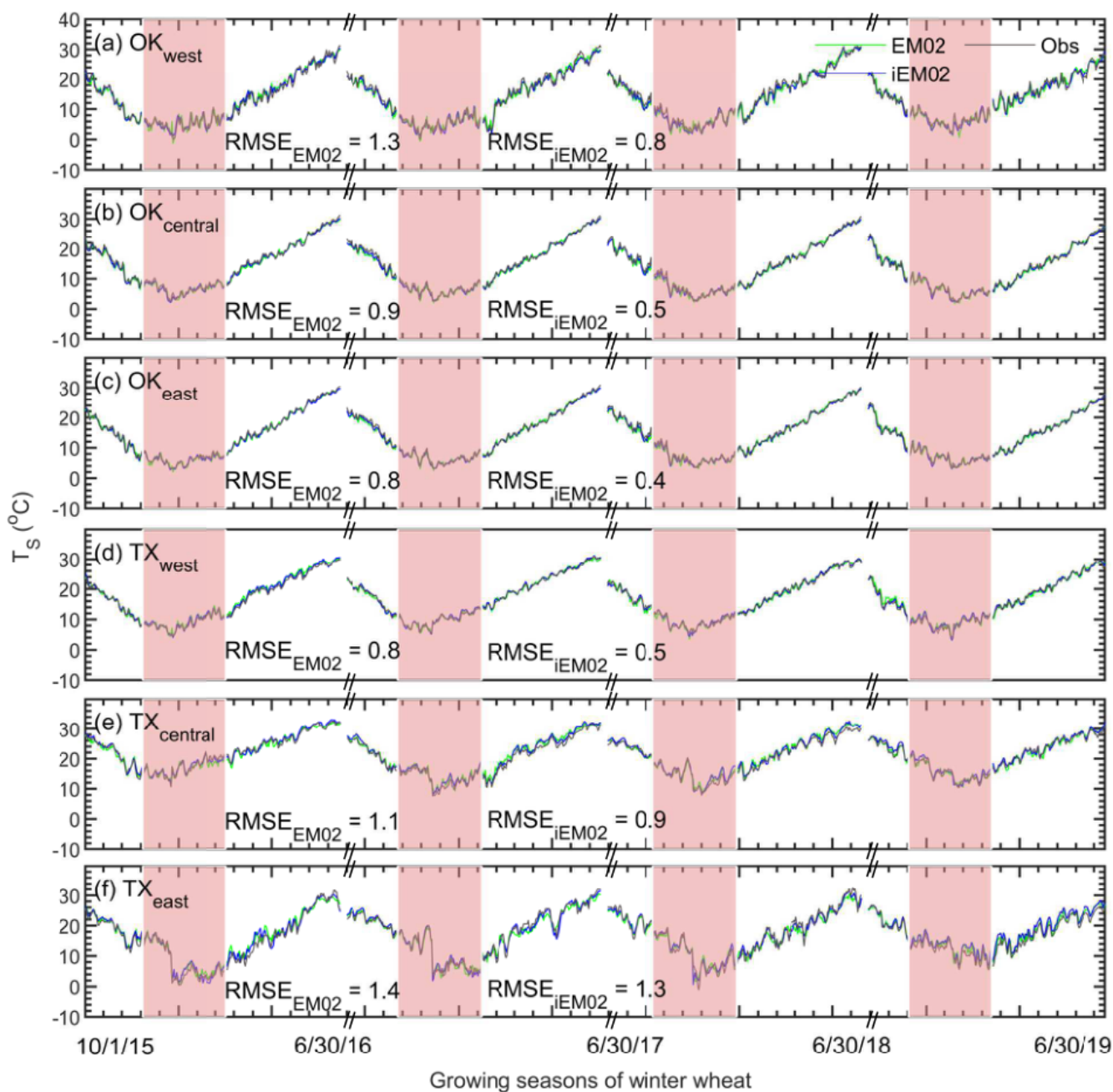


Figure 9: The same as Fig. 9 but for western, central, and eastern Oklahoma (a-c) and Texas (d-f).